Nanotechnology **19** (2008) 435303 (9pp) doi:10.1088/0957-4484/19/43/435303

Parallel-local anodic oxidation of silicon surfaces by soft stamps

Cristiano Albonetti[1], Javier Martinez[2], Nuria S Losilla[2], Pierpaolo Greco[1], Massimiliano Cavallini[1], Francesco Borgatti[1], Monica Montecchi[3], Luca Pasquali[3], Ricardo Garcia[2] and Fabio Biscarini[1]

[1] CNR-Istituto per lo Studio dei Materiali Nanostrutturati (ISMN), Via P Gobetti 101, I-40129 Bologna, Italy
[2] CSIC-Instituto de Microelectrónica de Madrid (IMM), Isaac Newton 8, 28760 Tres Cantos, Madrid, Spain
[3] Ingegneria dei Materiali e dell'Ambiente, Università di Modena e Reggio Emilia, Via Vignolese 905, I-41100 Modena, Italy

E-mail: c.albonetti@bo.ismn.cnr.it

Received 5 May 2008, in final form 4 August 2008
Published 22 September 2008
Online at stacks.iop.org/Nano/19/435303

Abstract
We investigate the fabrication of nanometric patterns on silicon surfaces by using the parallel-local anodic oxidation technique with soft stamps. This method yields silicon oxide nanostructures 15 nm high, namely at least five times higher than the nanostructures made with local anodic oxidation using atomic force microscopy, and thanks to the size of the stamp enables one to pattern the surface across a centimetre length scale. To implement this technique, we built a machine to bring the metallized polydimethylsiloxane stamp in contact with the silicon surface, subsequently inserted in a sealed chamber with controlled relative humidity. The oxide nanostructures are fabricated when a bias voltage of 36 V is applied between the stamp and the silicon for 2 min, with a relative humidity of 90%. The flexibility of the stamp enables a homogeneous conformal contact with the silicon surface, resulting in an excellent reproducibility of the process. Moreover, by means of two subsequent oxidations with the same stamp and just rotating the sample, we are able to fabricate complex nanostructures. Finally, a detailed study of the oxidation mechanism, also using a finite element analysis, has been performed to understand the underlying mechanism.

(Some figures in this article are in colour only in the electronic version)

1. Introduction

Anodic oxidation of silicon has been studied since 1977 [1]. Since then, numerous studies [2–6] have shown that anodic oxidation can produce thin and reproducible oxide layers on the silicon surface. This electrochemical process is simple, fast and performed at room temperature in ambient conditions, as opposed to the long and sophisticated procedure to grow thermal SiO_2 [7]. The anodic oxidation can be carried out in an electrolytic cell with organic solvents, such as a solution of KNO_3 in ethylene glycol with small amount of water [8], or pure water [9] as the source of electrolyte. These oxides, upon high-temperature annealing in He, exhibit fair electrical properties, albeit not comparable with those of the thermal oxides. In the course of time, the inability to reduce the porosity and improve the dielectric properties of these oxides has caused a decrease of interest in this topic. In the last decade, just a few articles devoted to this topic have appeared in the literature [10–13].

In the same period, a robust and versatile lithographic technique based on scanning probe microscopy (SPM) has emerged, namely local anodic oxidation. This technique has demonstrated the possibility to prototype ultra-small silicon oxide nanostructures with lateral size <50 nm and 1–4 nm high, with results comparable to state-of-the-art electron beam lithography [14]. This approach has been proven to be useful to fabricate nanoscale devices [15–17] or templates [18, 19], and to investigate electrochemical reactions in an attoliter

environment [15]. Local oxidation exploits the water meniscus formed between the tip and the substrate, when the tip is brought to a few nanometres above the surface. The tip (cathode)–water (electrolyte)–substrate (anode) electrolytic cell yields a nanometric sized oxidation of the substrate upon the application of a voltage bias across. Local anodic oxidation has the limitations of the SPM techniques, namely maximum scan size of the piezoelectric actuator (generally tens of microns) and the serial fabrication being dependent on the scan frequency.

Recently, several authors have scaled up the local oxidation process on silicon using a conductive stamp with multiple protrusions as a cathode. They follow the original idea of Jacobs [20] to increase the writing rate of the scanning probe lithography (serial process) by using a metallized stamp to oxidize a large surface area and fabricate more nanostructures at the same time (concept of parallel oxidation). Mühl *et al* [21] used a stamp with few protrusions to demonstrate the feasibility of parallel oxidation, Cavallini *et al* [22] transferred the bits of a metallized digital videodisk (DVD) to the silicon surface, and Martinez *et al* [23] used silicon stamps, modified by electron beam lithography, to generate arrays of parallel lines separated by 100 nm over cm^2 regions. In the above experiments, the areas oxidized are as large as 1 cm^2, and the heights of the oxide nanostructures are 3 nm, namely comparable to the ones fabricated by local anodic oxidation.

In this paper we demonstrate a relevant improvement of the parallel-local anodic oxidation process of silicon surface by combining the use of metallized soft stamps [20] with the pure-water-local anodic oxidation process. We have grown oxide nanostructures on the silicon surface up to 15 nm high, i.e. five times higher than those obtained with rigid or semi-rigid stamps. This process is stable, highly reproducible and allows the fabrication of different patterns with the same stamp, by simply changing the orientation of the sample.

2. Experimental results

The polydimethylsiloxane (PDMS) stamps (Sylgard 184 Down Corning) were prepared by replica moulding [24] using, as a master, the surface of a blank compact disk (CD), composed of an array of parallel lines with a periodicity of 1.4 μm, full width at half maximum (FWHM) 400 nm and height 200 nm. After the curing process, carried out for 1 h at 70 °C, the master replica is peeled off from the master and washed in pure ethanol to remove uncured polymer. Then the PDMS stamps were coated with a double-layer of metals by e-beam evaporation (adhesive layer of Cr-5 nm thick/layer of Au-50 nm thick) in a home-built high vacuum chamber (base pressure 8×10^{-8} mBar). The substrates are 1×1 cm^2 pieces of Si p- and n- doped, covered with a native silicon oxide layer (Siltronic, type n and p, 0.5 mm thick, orientation [100], resistivity $\rho \leqslant 0.0015\ \Omega$ cm— n type and $10 \leqslant \rho \leqslant 20\ \Omega$ cm— p type).

To bring the stamp into contact with the substrate, we built a machine [23] in which the stamp is fixed on a stamp-holder and moved downward by a micrometric screw, while the substrate is fixed to a rigid sample-holder (figure 1). The

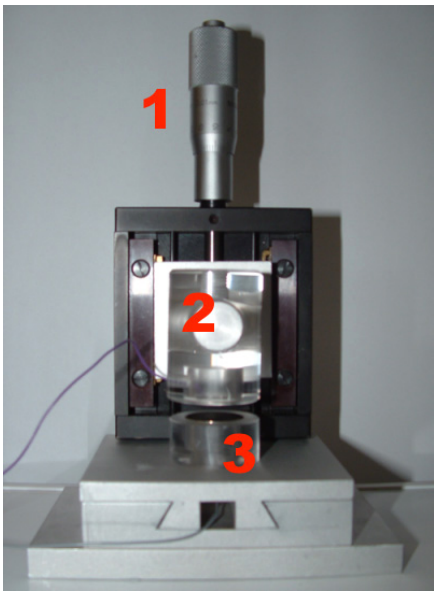

Figure 1. Machine to fabricate patterned surface by the parallel-local anodic oxidation process. The stamp is mounted on the sample-holder (2) and is moved downward by a micrometric screw (1) towards the substrate, pinned to a rigid sample-holder (3). Bias polarities: stamp (–), substrate (+).

PDMS stamps and the substrate are electrically connected to a voltage source (ELIND Model 3232). The machine was inserted inside a box (Tupperware, USA) with feed through for the bias and hygrometer's probe (PCE 313-A), in which the relative humidity (RH) is increased and controlled by bubbling pure water with nitrogen (water purified by a Milli-Q system ELGA PURELAB UHQ). When the RH reaches 90%, the stamp and the sample are gently placed in contact by means the downward motion of the micrometric screw. The stamp/water/silicon substrate system is an electrochemical cell in which the stamp is the cathode, the silicon substrate is the anode and the pure-water layer[4], adsorbed on the silicon and stamp surfaces, generates the electrolyte. When a bias voltage of 36 V DC is applied between the stamp and the substrate for 2 min, a pure-water anodic oxidation takes place at the anode. At the end of the oxidation process, a pattern of oxide lines is formed (figure 2(a)). The oxide lines height has been measured statistically by the height distribution graph (figure 2(b)), in which the difference between the positions of the peaks is the height of the oxide lines. The result obtained was 15 nm, about five times higher than for ones generated by parallel-local anodic oxidation using rigid stamps [23] or local anodic oxidation [15]. The oxide lines are 480 nm wide and, therefore, have low aspect ratio (1/32), as shown in the topographic profile (figure 2(c)).

Parallel-local anodic oxidation also works for stamps composed of motifs with different length scale as arrays of parallel lines with different periodicity (e.g. a replica of a blank DVD) and objects of different nanometric size (replica of a recorded DVD).

[4] The anodic oxidation works also with tainted water. The only one difference is the contaminants concentration in the oxide grown.

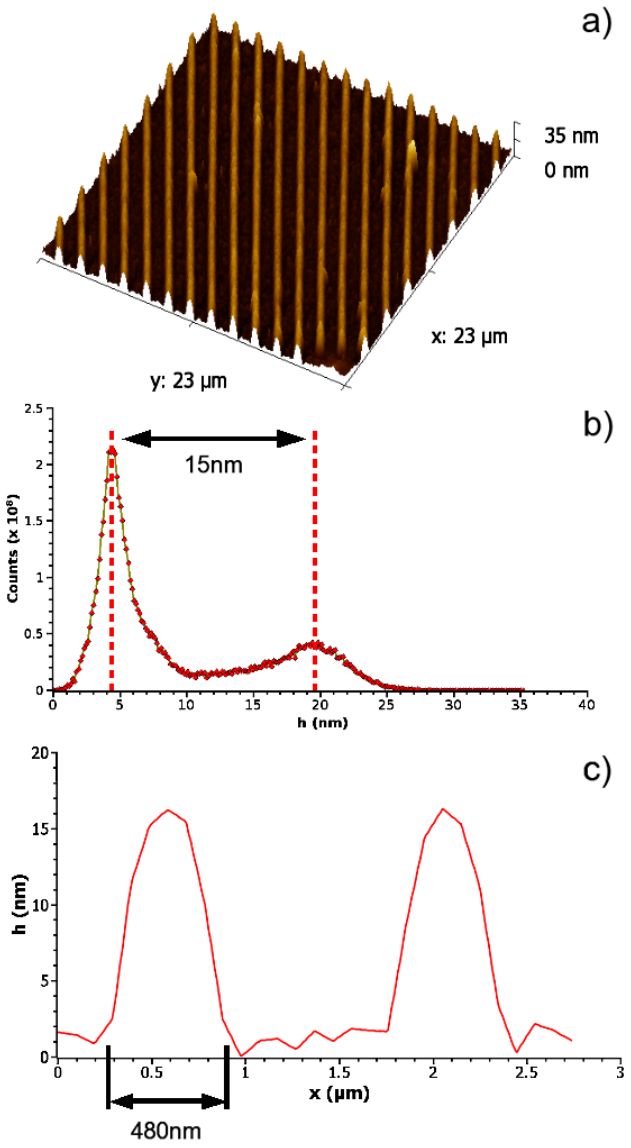

Figure 2. Oxide lines obtained over a silicon sample using a PDMS stamp after applying 36 V for 2 min. (a) 3D AFM (Smena, NT-MDT, Moscow, Russia) image of the oxide lines. (b) Height distribution graph of the topographic image (analysis done using the open source SPM software Gwyddion-www.gwyddion.net). The difference between the two peaks is the height of the oxide lines (15 nm). (c) Line profile of the AFM image.

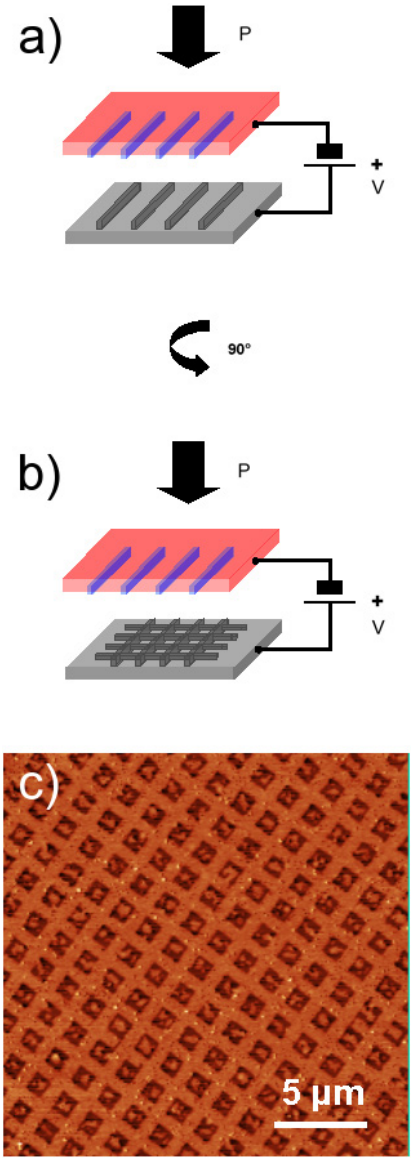

Figure 3. Oxidation sketch for fabricating complex patterns. The second oxidation, over a silicon sample previously patterned (a), produce a square pattern of crossed oxide lines just by turning the stamp 90° with respect to the oxide lines on the sample (b). (c) AFM image of the silicon sample after two sequential oxidations. The oxide lines were made by applying an electric field of 36 V for 2 min and are homogeneous for both oxidations.

The high reproducibility of this method is due to the breaking strength of the stamp that does not show any relevant degradation after several operations (up to 20). This is an important peculiarity property in order to repeat the process several times on the same sample and make more complex patterns. Figure 3 shows the pattern obtained after two successive oxidations with the same stamp on the same sample. The second oxidation is done over the first one (figure 3(a)), just turning the stamp by 90° in the plane (figure 3(b)). This operation generates a square pattern of crossed oxide lines (figure 3(c)). The first and second oxide stripes are similar, as a result of the reproducibility of the patterning process. It is noteworthy that the thickness of the SiO_x does not increase where the second oxide lines cross the first oxide lines. This suggests, in the first place, that the soft stamp can be conformally adjusted to the previous oxide pattern and that, on the intersections, the previous oxidation increases the electrical resistance and blocks the current flow.

Oxide nanostructure growth depends upon several experimental parameters: applied voltage V, oxidation time t, RH, and the applied force F. To make the oxidation procedure as reproducible as possible, we have investigated each parameter systematically.

V variable; $t = 2$ *min*, $RH = 90\%$ *and* F *fixed*. A constant voltage was applied across the electrodes and the flowing current was measured by an amperometer (Digital multimeter

Fluke 112) in series with the electrodes [2, 25]. The oxidation occurs when the stamp and the silicon are in contact and a voltage $\geqslant$30 V is applied. For these voltages circulates a current density $\geqslant$25 μA cm^{-2}, that is the minimum current useful to oxidize the silicon. Usually we applied 36 V with a circulating current varying, for different experiments, from 130 to 150 μA cm^{-2} (the current fluctuations are related to the applied force).

t variable; $V = 36$ *V*, $RH = 90\%$ *and F fixed*. The high current density flowing between the stamp and substrate makes the oxidation process fast and, therefore, the nanostructures are produced in less than 1 min [3].

RH variable; $V = 36$ *V*, $t = 2$ *min and F fixed*. The oxidation process occurs over all the range $10 \leqslant RH \leqslant 90\%$, but the RH values affect the height of the oxide lines. The graph in figure 4(a) shows two different regions (I and II) for the oxide lines heights obtained by varying RH systematically. In the range $10\% \leqslant RH \leqslant 40\%$ (region I), the height of the oxide lines is constant at $\approx$2 nm (the fit line shows a small increase of the height, just 0.01 nm per percentage unit of RH). On raising the RH (range $40\% < RH \leqslant 90\%$—region II), the height of the oxide lines increases to 15 nm, with a growth factor of 0.35 nm/% (as shown by the fit line). This behaviour, related to the thickness of the water layer adsorbed on the stamp and the silicon substrate, will be described in detail in section 3.

F measurements. A load cell [26] (RS-components 632-736) was used to measure the force applied by the stamp to the substrate. We fixed a conductive substrate (silicon substrate covered by 50 nm of Au) on the load cell cantilever, we brought the stamp (fixed on the stamp-holder) in contact with the substrate by the micrometric screw, and we measured the variation of the electrical resistance between the stamp and the substrate with respect to the displacement of the micrometric screw. At the same time, the downward movement of the micrometric screw bends the load cell cantilever (deflection of the cantilever expressed in V), so we are able to correlate the displacement of the micrometric screw with the force applied on the surface. The resistance–voltage–position graph (figure 4(b)) shows two different regions (I and II) separated by a dashed line. In region I, the resistance roughly follows an exponential decay, in agreement with the conformal adjusting of the PDMS stamp on the surface, while the deflection of the cantilever increases with a power law trend. When the stamp is conforming to the substrate (region II), the resistance graph shows a flat region (indicating a good electrical contact). The deflection of the cantilever is proportional to the force and follows a linear trend versus the displacement of the micrometric screw. Usually, the oxidation process has been realized when we are inside this flat resistance region. Here, the force applied from the stamp to the substrate ranges from 0.5 to 20 N.[5]

[5] The load cell measures a voltage V_{OUT} (V) proportional to the displacement of four strain gauges in a Wheatstone bridge (WB) configuration. $V_{OUT} = V_S k\varepsilon$, where $V_S = 12$ V is the WB voltage supply, $k = 2$ is the gauge factor and ε is the strain. ε is related to the stress σ by the Young's modulus E ($E_{PDMS} = 0.4$ MPa), $\sigma = E\varepsilon$. σ is a pressure $\sigma = F \cdot A^{-1}$, where F is the force (to measure) and A (stamp's area 7 mm $\times$ 7 mm) the surface under pressure. Finally $F = AEV_{OUT}(V_S k)^{-1}$.

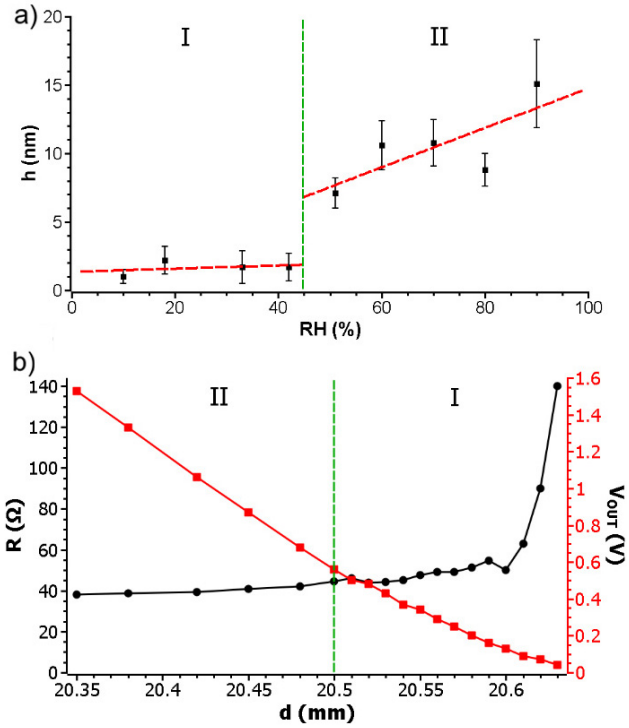

Figure 4. (a) Height of the oxide lines with respect to the relative humidity. In the range $10\% \leqslant RH \leqslant 40\%$ the height is fixed at $\approx$2 nm with a growth factor 0.01 nm/% (slope of the linear fit). In the range $40\% < RH \leqslant 90\%$, the height of the oxide lines increases from 7 to 15 nm with growth factor 0.35 nm/%. The error bars of the measurements are overestimated using the FWHM of the height distribution graphs. (b) Electrical resistance (Ω) between the stamp and the substrate measured by varying the displacement of the micrometric screw (mm) and corresponding output voltage of the load cell.

Chemical analyses are necessary to verify the quality of the oxide. We used two techniques: etching of the samples by means of a fluoridric acid (HF) solution [27], and analysis of the surface chemical composition by x-ray photoemission spectroscopy (XPS).

The oxide lines etched by HF solution (Sigma Aldrich) indicate that the nanostructures are made of silicon oxides. It was found that the etching rate of anodic oxide (64 Å s^{-1}) is much larger than that of thermal oxide [3] (4 Å s^{-1}). In addiction, measurements with a spectrophotometer have been performed to measure the anodic oxide thickness and its porosity. The average of the measured oxide thickness was 128 $\pm$ 2 Å, while its estimated refractive index was 1.3 (1.5 for thermal oxide [3]). As a consequence, the anodic oxide exhibits 30% more porosity than the thermal oxide.

The XPS measurements (Mg Kα source; $h\nu = 1253.6$ eV) were performed on patterned and unpatterned surfaces to understand how the pure water anodic oxidation process changes the chemical composition of the surface. Wide scan XPS spectra (figure 5(a)) clearly reveal the presence of C, O and Si at the surface. The presence of C is typical of samples not produced in ultra-high vacuum and is due to carbonaceous contamination. The peak of Au is absent, indicating that the stamp does not release gold clusters to the surface. In

particular, the detailed Si 2p spectra (figure 5(b)) evidence the chemical states of the Si atoms. The binding energies (BE) of the two peaks coincide with $Si0^+$ (BE $\sim$ 100 eV) and $Si4^+$ (BE $\sim$ 104 eV) valence states [28]. They indicate that the material probed by XPS is mainly composed of silicon and silicon dioxide (SiO_2).

Comparing the patterned and unpatterned silicon surfaces, the intensity of the Si peak is roughly halved, as expected from a sample with the surface covered approximately for the 50% by oxide lines high 10 nm. In fact, the typical XPS depth sensitivity to the chemical composition of the sample is of the order of $\sim 3\lambda$, where λ is the attenuation length of the photoelectrons escaping from the surface. For the Si 2p signal ($\lambda \sim 3$ nm) the depth sensitivity is $\sim$9 nm or lower than the height of the oxide lines (10 nm); therefore, in the patterned sample, the oxide lines screen the underlying Si signal. The surface coverage (50%) of the oxide lines is responsible for halving the Si contribution.

Further, the SiO_2 peak of the patterned sample exhibits a mild broadening with respect to the unpatterned sample, suggesting small contributions also from other Si chemical states ($Si3^+$, $Si2^+$, $Si1^+$). In conclusion, silicon oxides composed the nanostructures analysed.

3. Discussion

The oxide thickness is the most important difference between the oxide produced by rigid stamps and soft stamps. In this section, we propose and discuss the mechanism responsible for the oxide growth.

The morphology of the evaporated Au film on the PDMS stamp with periodic protrusions (array of parallel lines with periodicity 1.4 μm, FWHM 400 nm and height 200 nm) plays a central role in the oxidation mechanism. As numerically studied for block copolymer thin film [29], thin film deposited on a patterned surface (such as our Au film, 50 nm thick, deposited on the PDMS stamp) forms uniformly sized and spaced domains of material in correspondence of the protrusion edges. This phenomenon occurs when the film thickness is thinner than both the protrusion height (200 nm) and the separation between the protrusions (500 nm). For this reason, on the top of the stamp protrusions (figure 6(a)) there are formed two Au domains of small size, briefly called 'double protrusion' (figure 6(b) shows the line profile). The Au domains sizes are about 140 nm wide and 30 nm high each, and are separated by 250 nm (figure 6(c)).

To perform the oxidation process, the stamp is brought into contact with the silicon surface; therefore this double protrusion on top of the stamp lines creates nanometric size chambers with the surface (estimated volume for each line 9.6×10^3 nm$^2 \times 7 \times 10^3$ μm, where 7 mm is the typical lateral size of the stamp). The oxide lines produced with this stamp are homogeneous (figure 6(d)) and match the geometrical dimensions of the double protrusion structure (trapezoidal shape and base 450 nm wide—compare to the line profile of figure 2), except for the height, which is slightly smaller (15 versus 30 nm). To confirm this effect, a stamp without

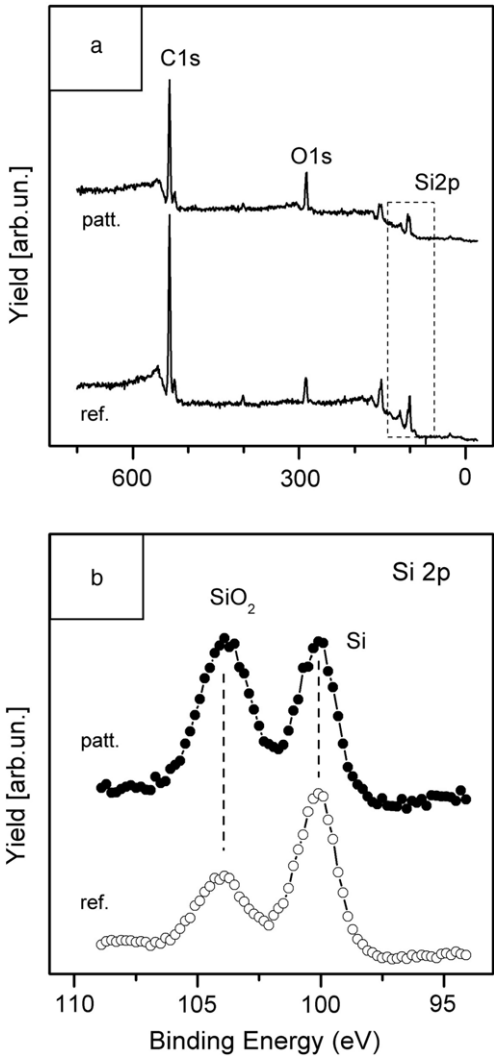

Figure 5. XPS spectra measured with a Mg Kα source (1253.6 eV). Panel (a): XPS wide scans of a reference silicon wafer with native surface oxidation and the patterned sample prepared by means of the PDMS stamp. Both XPS spectra show the contribution of carbon, oxygen and silicon. Panel (b): detail of the silicon 2p peak line shapes. The binding energies of the two peaks indicate the presence of different silicon chemical states, namely pure Si (BE 99.8 eV) and SiO_2 (BE 104 eV). The intensity of the SiO_2 peak for the patterned sample (filled circles) is roughly twice the one of the unpatterned silicon wafer (open circles).

double protrusions[6] was used to oxidize the surface using the same experimental parameters (V, t, RH and F). In this case, the oxidation has produced inhomogeneous lines, composed of oxide dots 2–3 nm high (in agreement with the Au film roughness on the stamp's lines) and aligned along the direction of the stamp protrusions (figure 6(d)).

These results are in agreement with experiments made by rigid [27] or semi-rigid [22] stamps and confirm that the oxidation process occurs under the stamp lines in the volume delimited by the double protrusions.

[6] The stamp without double protrusions is a result of an experimental mishap. The Au deposition was interrupted and resumed so the double protrusions were filled by the second evaporation.

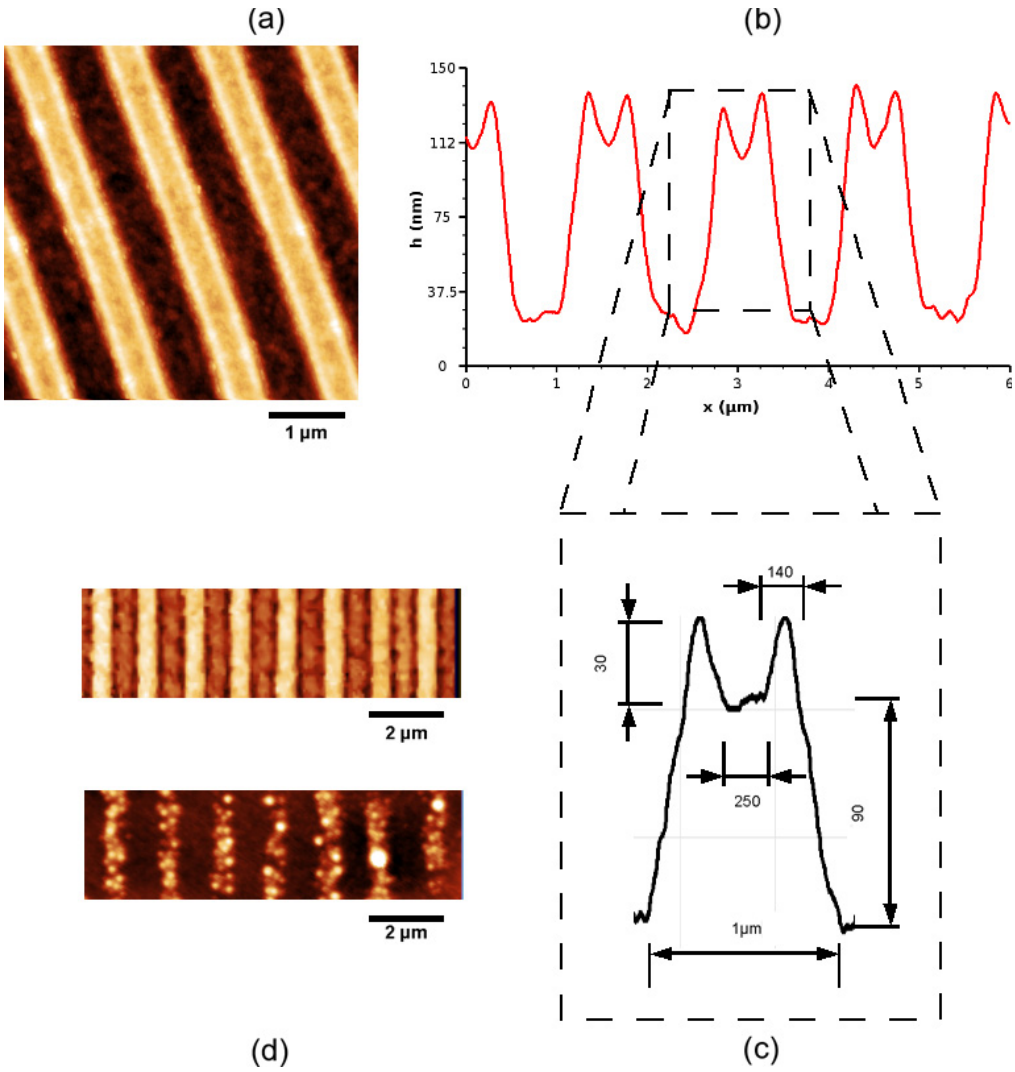

Figure 6. (a) AFM topographic image of the PDMS stamp's corrugations covered with evaporated Au and corresponding line profile (b) of the parallel lines (periodicity 1.4 μm, FWHM 400 nm and height 200 nm). (c) Transversal profile of one line with detailed dimension. The profile has been stretched out to increase the aspect ratio (1/10) and to stress the double protrusion shape. All the distances are in nm, except for the base line (in μm, as indicated). (d) AFM images of oxide lines produced by parallel-local anodic oxidation using a soft stamp with and without double protrusion. Note the oxide lines' homogeneity and inhomogeneity in the two cases, respectively.

From the experiments described above, it turns out that the height of the oxide lines increases with the RH. In particular, around $RH = 45\%$ there is sudden jump in the oxide height. This behaviour suggests a correlation with the volume of water adsorbed on the stamp and the substrate (expressed by RH) and the oxidation mechanism [30]. The contact between the double protrusion and the silicon surface creates a nanometric confined space where water condenses preferentially, owing to the higher local curvature (figure 7(a)). This acts as an electrolytic cell in which the metallized stamp is the cathode, the silicon surface is the anode and the pure water trapped in empty space is the electrolyte. As defined by Hung [3], this is a nanometric anodic oxidation reactor.

Thanks to the flexibility of the PDMS stamp, the stamp protrusions get deformed for a better adjustment with the silicon surface and the water squeezed between the double protrusions to partially fill the electrolytic chamber (figure 7(b)). In this condition, the oxide growth is not limited by the presence of the stamp, thus it can grow until its electrical resistance stops the electrochemical oxidation. A stamp without double protrusions does not trap the water, and produces inhomogeneous lines (figure 7(c)).

The force applied to the stamp during the oxidation process affects the spatial order of the patterned oxide nanostructures. In particular, with high force applied to the stamp, little oxide regions grow between the lines (figure 8(a)). This phenomenon is related to the deformation of stamps: when a high force is applied to improve the conformal contact with the surface, the stamp sags or collapses. We have simulated, by finite element analysis (Comsol Multiphysics® COMSOL, Lund, Sweden), the deformation stamp, varying the external load L applied to explain the growth of the little oxide regions between the lines.

The PDMS stamp has been carefully designed and modelled by coupling the PDMS replica (Young's modulus $E = 0.4$ MPa) with a gold thin film [29] ($E = 69$ MPa),

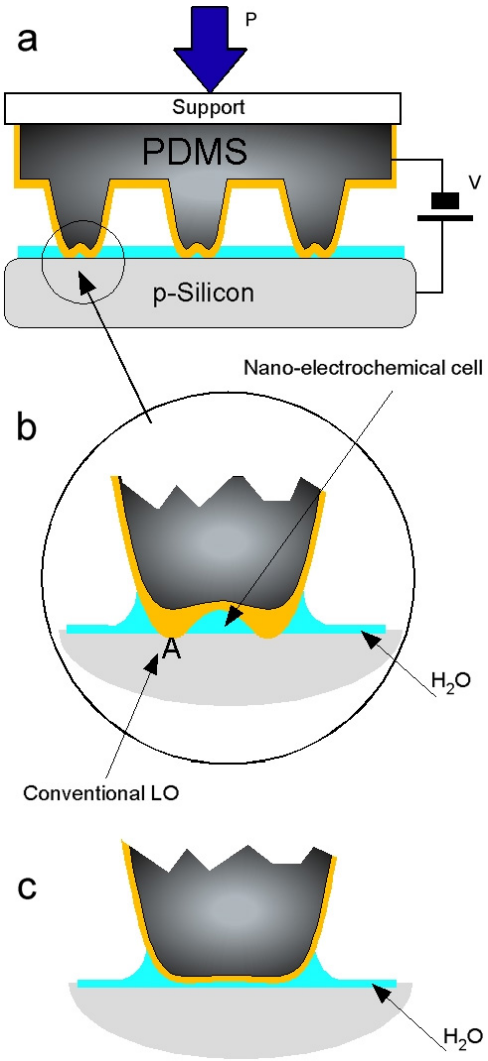

Figure 7. Scheme of the oxidation mechanism made by parallel-local anodic oxidation. (a) The stamp is put in contact with the surface with a pressure P; (b) the double protrusions of the stamp create a nanometric enclosed space filled by the water absorbed on the surface; (c) stamps without protrusions produce inhomogeneous oxide lines with small height.

whose mechanical response is sensibly different from that of PDMS. The stamp used for the simulation is a cross-section of a CD replica (periodicity 1.4 μm) with dimensions 500 μm $\times$ 100 μm, to take into account the strain energy dissipated in the 'bulk' part of the stamp. The stamp's surface is covered with 50 nm of Au and placed in conformal contact with the silicon substrate. The roughness of the Au surface (3 nm) has not been considered, being undistinguishable on the scale chosen for calculation. The boundary conditions used for the calculation were the standard static constraints of structural mechanics. A uniform load force L (expressed in N m^{-1}) has been applied on top of the stamp and varied to obtain the different configurations of the deformed stamp.

In the case of low L, e.g. 400 N m^{-1} (L is applied on a square stamp of width 7×10^{-3} m, corresponding to $F = 400 \times 7 \times 10^{-3} \approx 3$ N), the compression of the stamp does

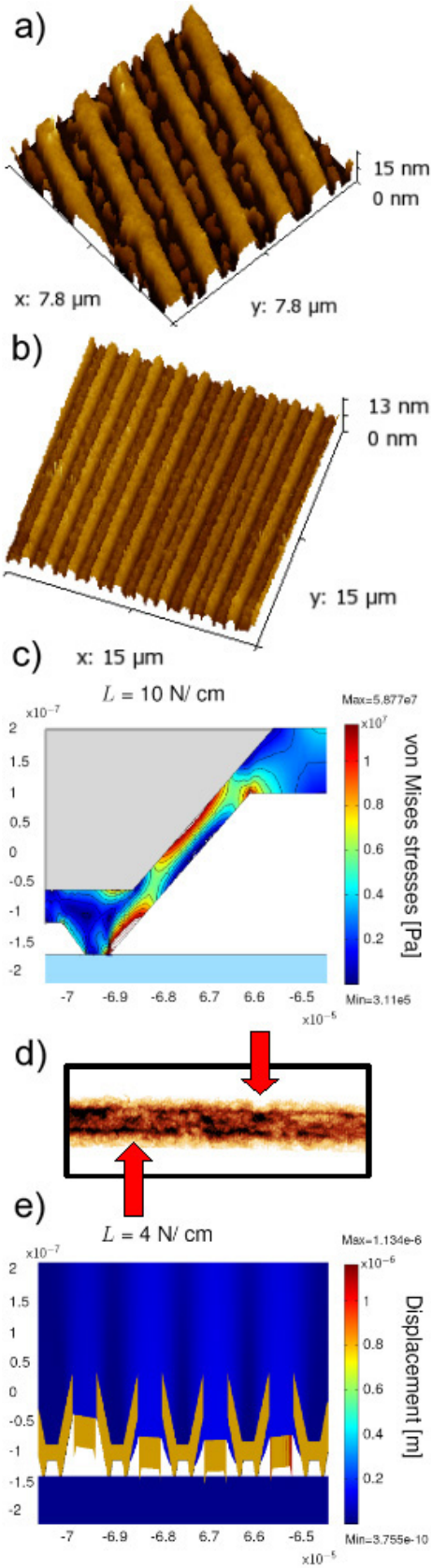

Figure 8. (a) 3D AFM topographic image of oxide lines with (a) and without (b) oxide regions between the lines; von Mises' stress map of the corner between the stamp's background and the protrusion base (c) and resulting fracture in the stamp (d) indicated by arrows; (e) simulated displacement of the modelled stamp with distribution of cracks on the Au film.

not yield any collapse of the structure. With this L value, the oxide lines grow homogeneously just under the stamp's lines; any oxide regions are present in between the lines (figure 8(b)).

Afterwards, the load L is increased to evaluate its minimum limit to create localized fractures in the stamp (also reported as the yield stress (f_s) measured by means of the von Mises' criterion (see footnote 6)). From the literature [30] (see footnote 6), the f_s reported for thicker gold films (100 nm–1 μm) is up to 150 MPa. In our condition, for a thinner film, we suppose an f_s of 20 MPa corresponding, for our experimental conditions, to $L = 100$ N m^{-1} ($F = 7$ N). The most solicited regions of the features are the corners between the stamp background and the base of the protrusion (figure 8(c)). This is confirmed by the topographic AFM image of a used stamp, where the fractures are exactly in the corner regions (figure 8(d)).

In agreement with these simulation and experimental results, we have assumed a distribution of cracks on the Au film and we have calculated the resulting displacement of the stamp. By applying $L = 50$ N m^{-1} ($F \approx 4$ N), we obtain a collapse of the 'channel ceiling', which is in contact with the substrate (figure 8(e)). This result explains the little oxide regions grown between the lines. As expected, the height of these oxide regions matches the roughness of the Au thin film.

4. Conclusions and perspectives

In conclusion, we have improved the patterning of silicon surfaces by parallel-local oxidation, combining the use of metallized soft stamps and the pure-water-local anodic oxidation process. This approach yields ordered arrays of nanometric structures of SiO_x, of unusual height (up to 15 nm). The use of stamps enables a large area patterning [31], and the elasticity of the PDMS allows multiple-step oxidation to create complex structures (e.g. grid). For these reasons, the parallel-local anodic oxidation turns out to be a versatile technique for nanofabrication.

The oxidation mechanism occurring in parallel-local anodic oxidation using soft stamps has been thoroughly investigated to control the experimental parameters and increase the reproducibility of the process. In particular, the experiments point out that the oxidation occurs inside the region confined between the double protrusions at the edge of stamp features and the surface. The study of the stamp deformation by using finite element analysis has been useful in understanding the origin of defects in the patterns.

Apart from the cited possible applications for parallel anodic oxidation (e.g. template [19]), these oxide patterns can be exploited as effective masters for replica moulding or nano-imprinting lithography. In this regard, we fabricated a PDMS stamp with nanometric channels, just 1 nm high and 450 nm wide, perfectly transferred from the patterned surface. Therefore, this approach can become a very versatile low cost and fast prototyping method, with easily renewed masters.

Acknowledgments

The authors wish to thank Mauro Murgia for the metallization of the stamps and Caterina Summonte for spectrophotometer measurements. The work was partially supported by EU integrated project NAIMO (No. NMP4-CT-2004-500355), MCyT (Spain) (MAT 2006-03833 and MAT2003-02655). ESF-EURYI DYMOT and 'PRRIITT NANOFABER' support MC and CA, respectively.

References

[1] Pliskin W A 1977 *J. Vac. Sci. Technol.* **14** 1064–81
[2] Jain G C, Prasad A and Chakravarty B C 1979 *J. Electrochem. Soc.* **126** 89–92
[3] Hung T F, Wong H, Cheng Y C and Pun C K 1991 *J. Electrochem. Soc.* **138** 3747–50
[4] Bardwell J A, Clark K B, Mitchell D F, Bisaillion D A, Sproule G I, MacDougall B and Graham M J 1993 *J. Electrochem. Soc.* **140** 2135–8
[5] Landheer D, Bardwell J A and Clark K B 1994 *J. Electrochem. Soc.* **141** 1309–12
[6] Clark K B, Bardwell J A and Baribeau J M 1994 *J. Appl. Phys.* **76** 3114–22
[7] Sze S M 1981 *Physics of Semiconductors Devices* (New York: Wiley)
[8] Mende G, Hensel E, Fenski F and Flietner H 1989 *Thin Solid Films* **168** 51–60
[9] Morfouli P and Pananakakis G 1989 *Phys. Status Solidi* a **111** 529–39
[10] Ohnishi K, Ito A, Takahashi Y and Miyazaki S 2002 *Japan. J. Appl. Phys.* **41** 1235–40
[11] Bensliman F, Fukuda A, Mizuta N and Matsumura M 2003 *J. Electrochem. Soc.* **150** G527–31
[12] Buttard D, Krieg C and Fournel F 2006 *Surf. Sci.* **600** 4923–30
[13] Nadji B 2007 *J. Mater. Proc. Technol.* **181** 230–4
[14] Calleja M, Anguita J, Garcia R, Birkelund K, Perez-Murano F and Dagata J A 1999 *Nanotechnology* **10** 34–8
[15] Garcia R, Martinez R V and Martinez J 2006 *Chem. Soc. Rev.* **35** 29–38
[16] Johannes M S, Cole D G and Clark R L 2007 *Nanotechnology* **18** 345304
[17] Kuramochi H, Ando K, Tokizaki T and Yokoyama H 2004 *Appl. Phys. Lett.* **84** 4005–7
[18] Xie X N, Chung H J, Liu Z J, Yang S W, Sow C H and Wee A T S 2007 *Adv. Mater.* **19** 2618–23
[19] Garcia R, Tello M, Moulin J F and Biscarini F 2004 *Nano Lett.* **4** 1115–19
[20] Jacobs H O and Whitesides G M 2001 *Science* **291** 1763–66
Jacobs H O and Whitesides G M 2002 *Patent Title: Electric Microcontact Printing Method and Apparatus* Pub. No.: WO/2002/003142, International Application No.: PCT/US2001/021151
[21] Mühl T, Kretz J, Mönch I, Schneider C M, Brückl H and Reiss G 2000 *Appl. Phys. Lett.* **76** 786–8
[22] Cavallini M, Mei P, Biscarini F and Garcia R 2003 *Appl. Phys. Lett.* **83** 5286–88
[23] Martinez J, Losilla N S, Biscarini F, Schmidt G, Borzenko T, Molenkamp L W and Garcia R 2006 *Rev. Sci. Instrum.* **77** 086106
[24] Cavallini M *et al* 2005 *Nano Lett.* **5** 2422–25
[25] Ghowsi K and Gale R J 1989 *J. Electrochem. Soc.* **136** 867–71
[26] Yegingil H, Shih W Y and Shih W-H 2007 *J. Appl. Phys.* **101** 054510
[27] Martinez R V, Losilla N S, Martinez J, Tello M and Garcia R 2007 *Nanotechnology* **18** 084021

[28] Himpsel F J, McFeely F R, Taleb-Ibrahimi A, Yarmoff J A and Hollinger G 1988 *Phys. Rev.* B **38** 6084–96
[29] Podariu I and Chakrabarti A 2000 *J. Chem. Phys.* **113** 6423–28
[30] Salvadori M C, Vaz A R, Melo L L and Cattani M 2003 *Surf. Rev. Lett.* **10** 571–5
[31] Innocenti M, Cattarin S, Cavallini M, Loglio F and Foresti M L 2002 *J. Electroanal. Chem.* **532** 219–25